Contrib Mineral Petrol (2000) 138: 1–16

R.J. Kinzler · J.M. Donnelly-Nolan · T.L. Grove

Late Holocene hydrous mafic magmatism at the Paint Pot Crater and Callahan flows, Medicine Lake Volcano, N. California and the influence of H_2O in the generation of silicic magmas

Received: 4 January 1999 / Accepted: 30 August 1999

Abstract This paper characterizes late Holocene basalts and basaltic andesites at Medicine Lake volcano that contain high pre-eruptive H_2O contents inherited from a subduction related hydrous component in the mantle. The basaltic andesite of Paint Pot Crater and the compositionally zoned basaltic to andesitic lavas of the Callahan flow erupted approximately 1000 ^{14}C years Before Present (^{14}C years B.P.). Petrologic, geochemical and isotopic evidence indicates that this late Holocene mafic magmatism was characterized by H_2O contents of 3 to 6 wt% H_2O and elevated abundances of large ion lithophile elements (LILE). These hydrous mafic inputs contrast with the preceding episodes of mafic magmatism (from 10,600 to ~3000 ^{14}C years B.P.) that was characterized by the eruption of primitive high alumina olivine tholeiite (HAOT) with low H_2O (< 0.2 wt%), lower LILE abundance and different isotopic characteristics. Thus, the mantle-derived inputs into the Medicine Lake system have not always been low H_2O, primitive HAOT, but have alternated between HAOT and hydrous subduction related, calc-alkaline basalt. This influx of hydrous mafic magma coincides temporally and spatially with rhyolite eruption at Glass Mountain and Little Glass Mountain. The rhyolites contain quenched magmatic inclusions similar in character to the mafic lavas at Callahan and Paint Pot Crater. The influence of H_2O on fractional crystallization of hydrous mafic magma and melting of pre-existing granite crust beneath the volcano combined to produce the rhyolite. Fractionation under hydrous conditions at upper crustal pressures leads to the early crystallization of Fe-Mg silicates and the suppression of plagioclase as an early crystallizing phase. In addition, H_2O lowers the saturation temperature of Fe and Mg silicates, and brings the temperature of oxide crystallization closer to the liquidus. These combined effects generate SiO_2-enrichment that leads to rhyodacitic differentiated lavas. In contrast, low H_2O HAOT magmas at Medicine Lake differentiate to iron-rich basaltic liquids. When these Fe-enriched basalts mix with melted granitic crust, the result is an andesitic magma. Since mid-Holocene time, mafic volcanism has been dominated primarily by hydrous basaltic andesite and andesite at Medicine Lake Volcano. However, during the late Holocene, H_2O-poor mafic magmas continued to be erupted along with hydrous mafic magmas, although in significantly smaller volumes.

R.J. Kinzler
Department of Earth and Planetary Sciences,
American Museum of Natural History,
Central Park West at 79th Street,
New York, NY 10024-5192, USA

J.M. Donnelly-Nolan
United States Geological Survey,
345 Middlefield Road, Menlo Park, CA 94025, USA

T.L Grove (✉) (tlgrove@mit.edu)
Department of Earth, Atmospheric and Planetary Sciences,
Massachusetts Institute of Technology (MIT),
Cambridge, MA 02139, USA

Editorial responsibility: J. Hoefs

Supplementary material Table 1e has been deposited in electronic form and can be obtained from http://link.springer.de/link/service/journals/00410.

Introduction

Medicine Lake volcano (MLV) is a large (~750 km^3) Quaternary shield volcano located in the southern Cascade Range, northern California. High MgO, high Al_2O_3 and low K_2O basalt (HAOT) are common around the flanks of the volcano, which has erupted throughout its more than half a million year history (Donnelly-Nolan 1988). This primitive tholeiitic basalt type has been shown to be parental to derivative andesitic magmas by FARM (fractional crystallization, assimilation, replenishment and mixing) processes (Grove et al. 1988; Baker et al. 1991). The tholeiitic basalt has also been demonstrated to be nearly anhydrous (H_2O < 0.2 wt%, Sisson and Layne 1993) and a product of melting of shallow mantle (Bartels

et al. 1991). However, trace element abundances for some higher K_2O and high MgO basalts at MLV suggest the existence of a calc-alkaline parental basalt as well (Bacon et al. 1997). This calc-alkaline parental basalt is characterized by elevated large ion lithophile element (LILE) abundances including Sr, Ba, and Rb, as well as by elevated $\delta^{18}O$. In this paper we use experimentally determined phase relations (Grove et al. 1982, 1997) to infer the H_2O content of the calc-alkaline basaltic and andesitic lavas at MLV. It is found that influxes of basaltic magma with elevated H_2O content (~3–6 wt%) occurred in late Holocene time and probably at earlier times in the history of MLV. Two late Holocene mafic lava flows, the Paint Pot Crater flow and the Callahan flow, display evidence that high water contents were involved in their generation. Chilled mafic inclusions in the youngest flows at MLV, the Glass Mountain rhyolite-dacite and the Little Glass Mountain rhyolite (Anderson 1933; Eichelberger 1975) also show evidence of high water contents (Grove et al. 1997). In addition, mineral compositions preserved in the Pleistocene Lake Basalt (Wagner et al. 1995) indicate pre-eruptive H_2O contents of 4 to 6 wt%. We discuss the significance of these high H_2O contents and explore the associated trace element and isotopic characteristics of the hydrous magmas.

Geology, chemical composition, and petrography of lavas

Analytical methods

Whole-rock major element analyses of basalts and andesites from the Paint Pot Crater and Callahan flows, as well as of inclusions from late Holocene rhyodacite and dacite lavas, were obtained by wavelength dispersive X-ray fluorescence spectroscopy at the US Geological Survey (USGS) laboratory in Lakewood, Colorado, USA. Trace elements amounts of selected lavas were analyzed by energy dispersive X-ray fluorescence at the USGS in Menlo Park and trace and rare earth elements were determined by neutron activation analysis at the USGS laboratories in Lakewood, Colorado, and Reston, Virginia, USA. Isotopic compositions of Sr were determined on the NIMA-B mass spectrometer at MIT and, for those samples, the abundances of Sr were obtained by isotope dilution. Grove et al. (1982) report the analytical procedures and uncertainties. Major and trace element concentrations, as well as isotopic compositions for selected lavas, are presented in Table 1. The abundances presented for the Callahan lavas in Table 1 are averages of the mapped groups (numbered from 1 to 5). The complete data set of individual analyses is presented as Table 1 in the Springer electronic supplementary material accompanying this manuscript and can be accessed at http: //link.springer.de. Sample locations are shown in Fig. 1 for the Callahan samples. Mineral compositions of lavas and inclusions were obtained with a five-spectrometer JEOL 733 Superprobe at MIT using online data reduction and matrix correction procedures of Bence and Albee (1968) with the modifications of Albee and Ray (1970). Selected mineral chemical data are presented in Table 2.

Geologic setting and compositional variation

The last 11,000-year history of volcanic activity at Medicine Lake is summarized in Donnelly-Nolan et al. (1990). Relative ages are shown in Fig. 2, with No. 1 the oldest and No. 17 the youngest. This numbering scheme will be retained in the present discussion. The Callahan and Paint Pot Crater flows (Nos. 14 and 15 respectively in Fig. 2) are the most recent mafic eruptions at the MLV. Previous petrological and geochemical studies (e.g., Smith and Carmichael 1968; Condie and Hayslip 1975; Mertzman 1977, 1979; Grove et al., 1982) of the MLV have reported data for the Callahan and Paint Pot Crater flows.

Basaltic andesite of Paint Pot Crater

The Paint Pot Crater lava flow (Fig. 2) has an estimated area of 2.7 km^2 and volume of 0.04 km^3; the volcano erupted near the western edge of the MLV about 1130 ^{14}C years B.P. It was partially buried in less than a century by white tephra of the nearby rhyolite of Little Glass Mountain, which erupted on a similar northeasterly trending vent. Four chemical analyses show only a small range of compositional variability (SiO_2 content varies from 52.9 to 53.2 wt%) and the average is reported here (Table 1, see electronic supplement for all four analyses). Two of the samples are from the same road cut near the southern end of the flow. The other two samples were collected near the top and bottom of a 1-m-thick tephra deposit located about 1 km NE of Paint Pot Crater. Additional samples collected from the Paint Pot Crater flow and analyzed at the University of Massachusetts (reported in Table 1) show no evidence of significant compositional variation within the flow. Two partially melted granitic inclusions have been found in the unit along with a trace amount of centimeter-size mafic crystal clots.

Basaltic andesite and andesite of the Callahan flow

The Callahan flow (Fig. 2) is only slightly older than the Paint Pot Crater flow, with an age of about 1150 years ^{14}C years B.P. (Donnelly-Nolan et al. 1990). Tephra from the Paint Pot Crater eruption immediately overlies uneroded Callahan tephra, substantiating the fact that there was only a short time interval between eruption of the two flows. The unit covers about 23 km^2 and the total erupted volume is about 0.33 km^3. The Callahan flow probably erupted continuously from closely spaced vents at and near Cinder Butte over a period of time ranging from a few months to perhaps a few years. It consists of five lobes with successively decreasing silica content that have been mapped separately and are shown in Fig. 1. An accompanying tephra deposit has been found as far as 15 km from the vent area (C.D Miller, unpublished data).

Five compositional and spatial subsets of the lava have been identified (Fig. 1; Table 1). The group 1 andesite ranges from 57.4 to 58.0% SiO_2 and represents about half the erupted volume (Fig. 3). Eruptive volume declined as SiO_2 content decreased. The height of the flow front also declined with SiO_2 content as the erupted lava became progressively more fluid. The group 5 basalt

Table 1 Major element compositions of average Callahan lava groups and representative trace, rare earth and isotopic compositions of Callahan and Paint Pot Crater lavas and related samples. Major element XRF analyses were done at US Geological Survey (USGS) laboratories in Lakewood, CO (analysts: J. Baker, A.J. Bartel, J.S. Mee, R.V. Mendes, D.-F. Siems. K. Stewart, J. Taggart, and J.S. Wahlberg), and Menlo Park, CA (analysts: L. Espos, T. Fries, S.T. Pribble, and D. Vivit). Trace element analyses (Rb, Sr, Y, Zr, Nb, Ba,-Ni) were performed using a Kevex energy-dispersive XRF system at USGS laboratories in Menlo Park, CA, by P. Bruggman, T. Frost, J.R. Lindsay, and D. Vivit. Rare earth elements, Th, and U were obtained by instrumental neutron activation analysis at USGS laboratories in Lakewood, CO (analysts J. Budahn, R. Knight, D.M. McKown, and H.T. Millard) and Reston, VA (analysts P. Baedecker, J. Mee, C.A. Palmer, and G. Wandless). See text for analytical methods. Isotopic analyses were performed at Massachusetts Institute of Technology by R-.J. Kinzler. Typical standard errors for the Sr isotope ratios is (2σ) 0.003%

	Callahan flow group averages				Inclusions			Paint Pot		Glass Mt. inclusions	
	1	2	3	4	5	1396M Tephra	83–23b	901Ma	41M	1140Mf	1544M
SiO_2	57.49	56.16	55.53	54.10	52.48	55.8	49.0	74.3	52.8	56.3	52.3
Al_2O_3	17.05	17.31	17.37	17.73	17.72	17.0	18.50	13.10	18.5	17.4	19.4
FeO*[a]	6.82	7.18	7.35	7.74	8.31	7.59	8.20	1.13	8.22	7.17	6.60
MgO	4.80	5.25	5.47	5.88	6.52	4.83	11.30	0.10	6.73	4.42	7.66
CaO	7.39	8.01	8.24	8.83	9.65	8.21	9.90	0.56	9.37	7.88	9.34
Na_2O	3.73	3.59	3.58	3.50	3.32	3.66	2.29	4.00	3.18	3.54	2.91
K_2O	1.53	1.29	1.22	0.96	0.68	1.18	0.55	4.63	0.69	1.26	0.75
TiO_2	0.87	0.90	0.92	0.94	0.99	1.03	0.48	0.13	0.83	0.95	0.61
P_2O_5	0.18	0.17	0.18	0.17	0.18	0.20	0.43	0.0	0.17	0.18	0.13
MnO	0.13	0.13	0.14	0.14	0.15	0.14	0.03	0.02	0.13	0.12	0.11
Total						99.66	100.04	98.3	99.80	99.22	99.81
LOI						1.49	–	1.07	–	0.29	< 0.01
La	12.3	11.2	10.5	9.3	8.2		5.1	35.1	9.1	13	8.11
Ce	25.8	23.8	23.0	19.7	18.1		10.5	66.3	19.1	27	16.7
Nd	13.5	12.9	12.9	11.4	10.7		5.2	29.0	12.5	14	9.2
Sm	3.53	3.45	3.40	3.25	3.24		1.64	6.45	3.05	3.74	2.35
Eu	1.04	1.03	1.05	1.03	1.05		0.52	0.34	0.93	1.1	0.75
Tb	0.66	0.63	0.61	0.58	0.61		0.29	1.20	0.52	0.65	0.35
Yb	2.58	2.47	2.56	2.42	2.40		1.24	4.59	2.09	2.2	1.24
Lu	0.38	0.38	0.36	0.38	0.37		0.19	0.70	0.31	0.3	0.18
Rb	45	36	40	25	16		16	122	14	41	30
Sr	323	322	338	346	357		364	46	421	442	484
Y	26	26	26	25	27		11	41	18	21	16
Zr	147	132	134	122	111		66	174	100	132	91
Nb	6	6	6	6	6		–	13	3	4	7
Ba	386	331	313	283	214		156	608	256	369	228
Ni	54	59	65	58	67		240	–	90	25	168
Th	4.5	3.6	3.3	2.3	1.2		1.6	12.7	1.58	3.4	
U	1.7	1.4	1.3	0.92	0.40		0.50	4.02	0.50		
$^{87/86}Sr$	0.70372			0.70367	0.70371		0.70386		0.70373	0.70386	0.70384

[a] FeO* is Fe calculated as FeO, *LOI* is loss on ignition. See Table 1 (electronic supplementary table) for complete data set

represents only 1% of the erupted volume and covers 1 km^2. Silica content of this last erupted group ranges from 51.8 to 53.3%. Additional samples (Table 1) were used in constraining the distribution of the five lava groups shown in Fig. 1.

A tephra sample collected in a small depression on top of group 1 lava has a composition between group 1 and group 2 samples (sample 1611M). A tephra sample collected on top of group 2 lava (1783M) is similar in composition to group 3 lava. No Callahan tephra was found on top of group 3, 4, or 5 lava. A tephra sequence about 1 m thick located just east of the flow yielded all the additional tephra samples analyzed. Two samples collected near the base of the deposit are strongly enriched in TiO_2 and FeO^t; the other samples lie compositionally between group 1 and group 2 lavas. We suggest that an early relatively explosive phase of the eruption began after half of the emplaced lava had already erupted as group 1 lava. Eruptions that scattered tephra beyond the vent area apparently ended by the time group 3 lava erupted.

Samples of bombs and cinders collected from Cinder Butte have an SiO_2 content ranging from 52.7 to 55.5%, overlapping the compositions of groups 2 through 5, and suggesting that the cone continued to be active during much of the eruption. The lack of Cinder Butte samples with group 1 compositions could indicate that early near-vent cinders were buried as the cone grew during the Strombolian activity. Melted silicic inclusions are relatively common in Cinder Butte; two were analyzed and are listed in Table 1. They have compositions similar to a nearby older rhyolite flow. In addition, one cumulate mafic inclusion has been found in the flow (sample 83–23b, Fig. 1; Table 1).

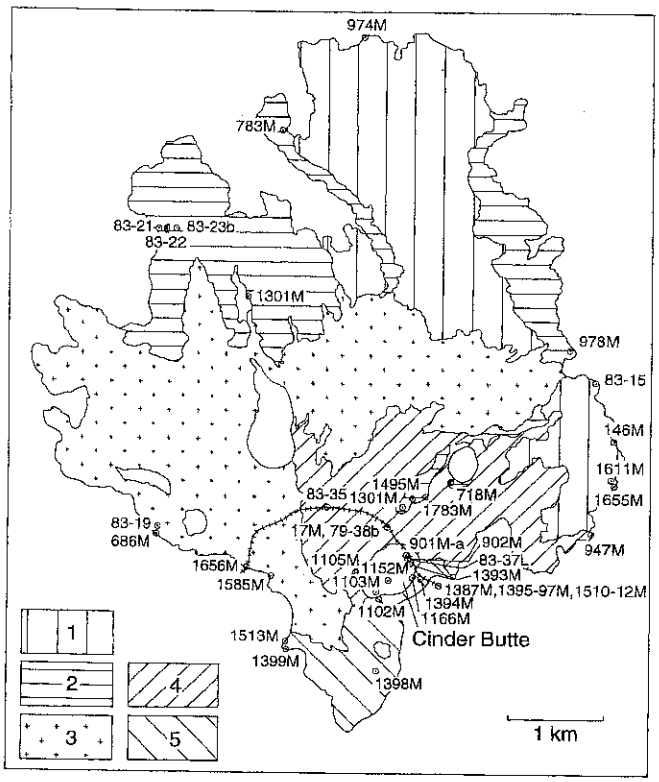

Fig. 1 Map of the compositionally-zoned Callahan flow. Patterns indicate composition groups. Group 1 lava erupted first and is highest in SiO_2 content; group 5 erupted last and is lowest in SiO_2. Analyses are in Table 1. *Hachured line* is old railroad grade, now a road that provides access to the flow

Petrography

Paint Pot Crater flow

The lavas of the Paint Pot Crater flow contain approximately 5 vol% phenocrysts of plagioclase and olivine. Plagioclase is more abundant than olivine. These phases are present as isolated euhedral phenocrysts from 0.5 to 2 mm in length, as glomerocrystic intergrowths (Fig. 5A) and as elongate and/or glomerocrystic blobs up to 5 cm in the longest dimension. Melt inclusions are present in the olivine (Fig. 5A) and contain hydrous glass, amphibole, pyroxene and an unidentified Ca-Al-Si mineral. Compositions of the minerals present as glomerocrystic intergrowths and inclusions are plotted in Fig. 4. The representative mineral compositions and compositions of the assemblages trapped in the melt inclusions are reported in Table 2.

Callahan flow

The lavas of the Callahan flow contain between 1 and 5 vol% phenocrysts. Plagioclase is the dominant phenocryst phase and ranges from 1 to 2 mm. Olivine (1 to 2 mm) is present in all samples, but greatest in abundance in the group 5 lavas. Orthopyroxene and rare high Ca-clinopyroxene grains (≥1 mm) are also present in most of the lavas, and their abundance increases with increasing bulk rock SiO_2 content. The Callahan lavas are texturally diverse and range from nearly aphyric, intersertal textured basalts with rare microphenocrysts of olivine and plagioclase to andesites with phenocrysts of plagioclase, olivine and orthopyroxene set in a pilotaxitic groundmass. Textural features characteristic of magma mixing are present in the groups 1–4 Callahan lavas. Textures indicate resorption of plagioclase and orthopyroxene phenocrysts as a result of magma mixing (see Fig. 3 of Gerlach and Grove 1982). The minerals are not in equilibrium with the enclosing magma and indicate the presence of a mafic, Mg-and Ca-rich end member liquid and an evolved Fe- and Na-rich end member liquid(s) (see Figs. 4 and 5 of Gerlach and Grove 1982). To provide constraints on the conditions of fractional crystallization in the Callahan magmatic system, a systematic survey of the compositional variations among olivine + plagioclase and pyroxene + plagioclase glomerocysts was undertaken. The compositions are shown in Fig. 4 and reported in Table 2. These compositions are from the cores of intergrown minerals that appear to have co-crystallized.

Discussion

Compositional variations in the Callahan flow

The group 1–5 lavas of the Callahan flow show a consistent relation between age and chemical composition. Each successively younger batch of lava was less evolved, and this relation holds for both major and trace elements (Fig. 6). Element to element co-variation define linear trends, with some notable exceptions (e.g., FeO-MgO, Fig. 6). The variations in incompatible element abundances are significantly larger than those expected from fractional crystallization (Fig. 7). When this is combined with the observation that the lavas contain disequilibrium phenocryst assemblages, it can be strongly argued that a magma mixing process occurred (Grove et al. 1982). The tephra samples depart from the linear trends that characterize the compositional variation in the lava flows, and indicate that the mixing must have involved more than two end members. The compositionally zoned Giant Crater lava field (Baker et al. 1991) and the mixed Burnt Lava flow (Grove et al. 1988) generally show similar characteristics that can be accounted for by a process that involves mixing of the following end members: (1) a shallow, anhydrous, iron-rich fractionate from a primitive basaltic parent, (2) a granitic crustal component and (3) a primitive, anhydrous basaltic parent. However, as demonstrated below, the process that generated the compositional variations of the Giant Crater lava field and the Burnt Lava flow fails to produce the petrological and geochemical variations observed in the Callahan lavas.

Table 2 Compositions of minerals in Callahan and Paint Pot Crater lavas and melt inclusions in Paint Pot Crater lava. Mineral analyses are from cores of grains that appear to have crystallized simultaneously

Sample	83–18[a]		83–23a		83–23b			83–14a	
	ol[b]	pl	ol	pl	ol	pl	cpx	opx	pl
SiO_2	39.6	46.4	37.7	49.7	38.8	48.2	51.7	51.6	57.1
Al_2O_3	0.0	34.1	0.0	31.3	0.0	33.5	3.17	0.86	25.7
TiO_2	0.04	–	0.08	–	0.0	–	0.71	0.62	–
Cr_2O_3	0.08	–	0.0	–	0.14	–	0.64	0.09	–
FeO	15.3	0.36	26.7	0.76	19.4	0.52	7.00	24.4	0.40
MnO	0.22	–	0.36	–	0.29	–	0.13	0.47	–
MgO	45.9	0.14	35.7	0.15	42.0	0.12	16.3	19.8	0.03
CaO	0.19	17.6	0.32	15.6	0.20	16.9	20.5	2.00	9.45
Na_2O	–	1.43	–	2.68	–	1.97	0.29	–	6.05
K_2O	–	0.02	–	0.11	–	0.05	–	–	0.38
Sum	101.3	100.1	100.9	100.3	100.8	101.3	100.4	99.8	99.1
Mg# or An	84.2	87.1	70.4	75.8	79.4	82.3	80.5	59.2	45.3

	79–24e[c]	79–24e Melt inclusion[e]						
	ol	pl	ol[d]	gl	amp	cpx	Ca-Al	sp
SiO_2	40.1	46.0	39.3	63.1	42.4	48.3	25.2	0.0
Al_2O_3	0.0	33.8	0.0	20.2	13.9	6.64	20.8	56.6
TiO_2	0.01	–	0.0	0.14	2.22	0.84	4.81	0.17
Cr_2O_3	0.05	–	0.02	0.0	0.07	0.05	0.0	0.26
FeO	14.0	0.80	14.2	1.05	10.8	8.66	24.2	26.3
MnO	0.25	–	0.18	0.05	0.19	0.22	0.09	0.16
MgO	46.6	0.17	45.7	0.42	15.0	14.4	11.5	15.8
CaO	0.17	17.4	0.17	4.30	10.9	20.6	12.0	0.0
Na_2O	–	1.42	–	5.09	2.38	0.13	0.58	–
K_2O	–	0.00	–	1.05	0.11	–	–	–
Sum	101.2	99.6	99.6	95.4	98.0	99.8	99.2	99.3
Mg# or An	85.6	87.1	85.2	41.2	71.2	74.7	45.9	51.7

[a] 83–18 is a group 5 Callahan lava; ol + pl intergrowths. 83–23a and 83–23b are group 2 Callahan lavas; ol + pl and ol + pl + cpx intergrowths. 83–14a is group 1 Callahan; opx + pl intergrowth; analyses of unreacted cores

[b] *ol* Olivine, *pl* plagioclase, *cpx* high-Ca clinopyroxene, *opx* orthopyroxene, *gl* glass, *amp* amphibole, *Ca-Al* unknown silicate mineral in melt inclusion

[c] ol + pl intergrowth in Paint Pot Crater sample 79–24e (see Gerlach and Grove 1982 for analysis of an equivalent sample, 79–24c)

[d] ol host of melt inclusion in 79–24e

[e] Inclusion and minerals shown in Fig. 5

Comparison of Callahan lavas with experimentally produced liquid lines of descent

A comparison of the compositional trends expected for fractional crystallization of liquids similar to the Callahan lavas provides insight into the processes that led to the observed compositional variability. Experimental data are available at 0.1 MPa from anhydrous crystallization experiments on 79–38b (Grove et al. 1982; Grove and Juster 1989), a group 4 Callahan lava, and from experiments on H_2O- saturated Medicine Lake basalts and andesites at 100–200 MPa (Sisson and Grove 1993a, b; Grove et al. 1997). The compositions used in the Grove et al. (1997) experiments (1140Mf and 1544M) are similar to the group 3 Callahan lavas (Table 1). Oxygen fugacity was controlled near the quartz-fayalite-magnetite (QFM) buffer for the anhydrous, 0.1 MPa experiments on composition 79–38b, and at the nickel-nickel oxide (NNO) buffer for the H_2O-saturated experiments at 100–200 MPa.

The Callahan lavas are characterized by elevated and near constant Al_2O_3 (17–18 wt%, Fig. 8A), a slight decrease in TiO_2 (Fig. 8B), and a continuous decrease in FeO (Fig. 8C), with decreasing MgO. The liquid line of descent followed during crystallization at shallow anhydrous conditions shows the influence of a high ratio of plagioclase to mafic silicates (olivine and pyroxenes) which leads to a decrease in Al_2O_3 and increase in FeO and TiO_2 with decreasing MgO (Grove and Kinzler 1986). In contrast, crystallization under hydrous conditions is characterized by a lower ratio of plagioclase to mafic silicates and earlier appearance of Fe-Ti oxides in the crystallizing assemblage. These result in a nearly constant Al_2O_3 and decrease in FeO and TiO_2 with decreasing MgO. Variations in oxygen fugacity will not modify the Al_2O_3 variations that occur under anhydrous conditions but might be anticipated to affect the FeO and TiO_2 variation during crystallization. However, the effect of variations in oxygen fugacity has been investigated by Grove and Juster (1989). These authors found FeO and TiO_2 enrichment similar to that shown in Fig. 8 in experiments on 79–38b conducted under extremely oxidizing conditions (two orders of magnitude more oxidizing than NNO and NNO + 2). Thus, the

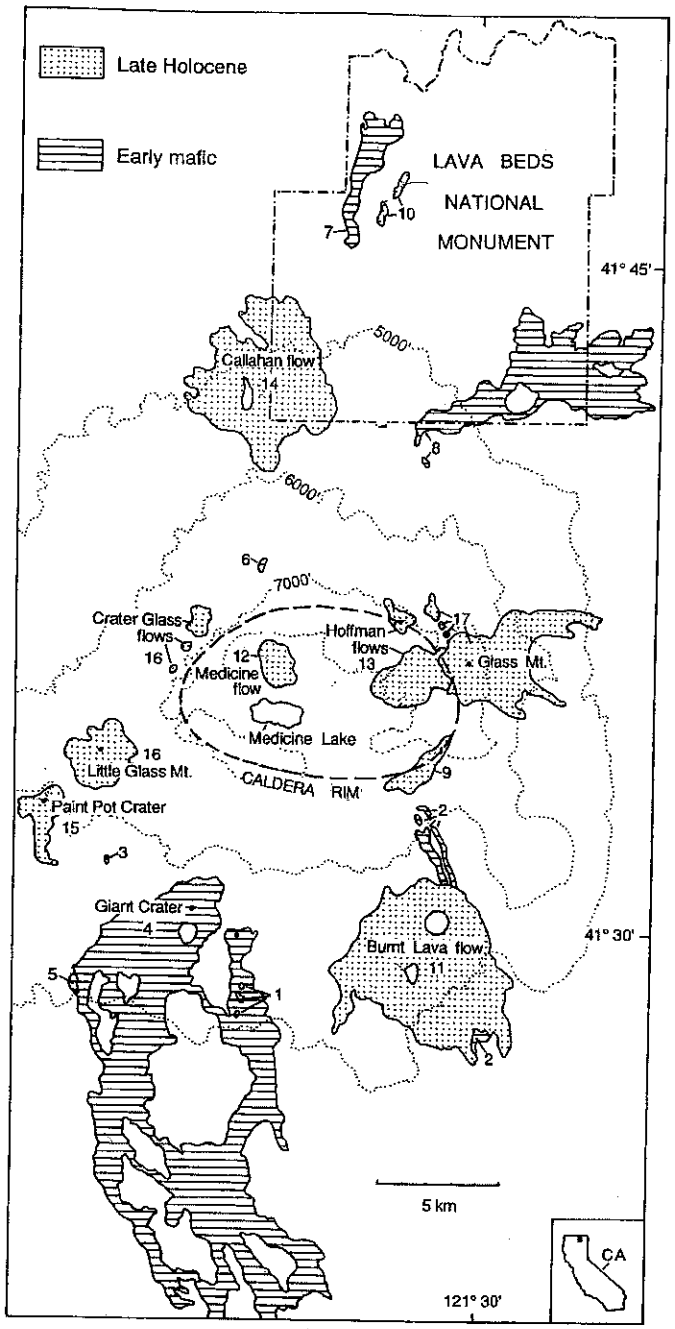

Fig. 2 Location map of the most recent lavas at Medicine Lake volcano. The earliest eruption is *No. 1*; the latest is *No. 17*. Early mafic eruptions (*Nos. 1–8*) are basalt and basaltic andesite about 10,600 years old (Donnelly-Nolan et al. 1990). Giant Crater lavas extend about 25 km further south than shown. Late Holocene lavas are *Nos. 9–17*. Flow *No. 9* is the andesite of the Pit Crater (4300 ^{14}C years B.P.) and flow *No. 10* is the basalt of Ross Chimneys and Black Crater

closest match to the Callahan trend is provided by the hydrous crystallization experiments. As discussed above, however, the variations in the abundance of incompatible elements (Fig. 7) are significantly different from those expected for fractional crystallization, implying that fractional crystallization alone cannot reproduce

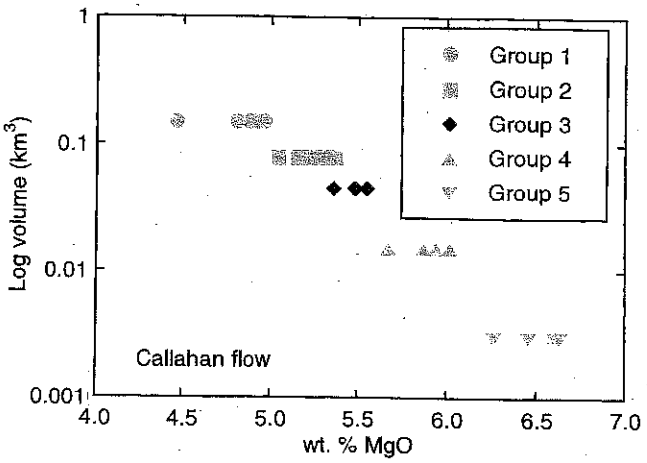

Fig. 3 Log volume (km^3) vs. MgO plot of Callahan lavas showing a nearly linear relationship. Only group 1 lavas fall slightly off the trend, perhaps reflecting the difficulty of estimating their volume due to coverage by younger lavas

the Callahan lava compositional trends. For example, the Rb, Ba and Th abundances in group 1 lavas are approximately two times higher than expected for fractional crystallization of a group 5 parent.

Compositional variations of minerals in Callahan and Paint Pot Crater lavas

The compositional variation of co-existing minerals provides additional information on the conditions of crystallization of the Callahan and Paint Pot Crater lavas. Variations in the composition of co-existing

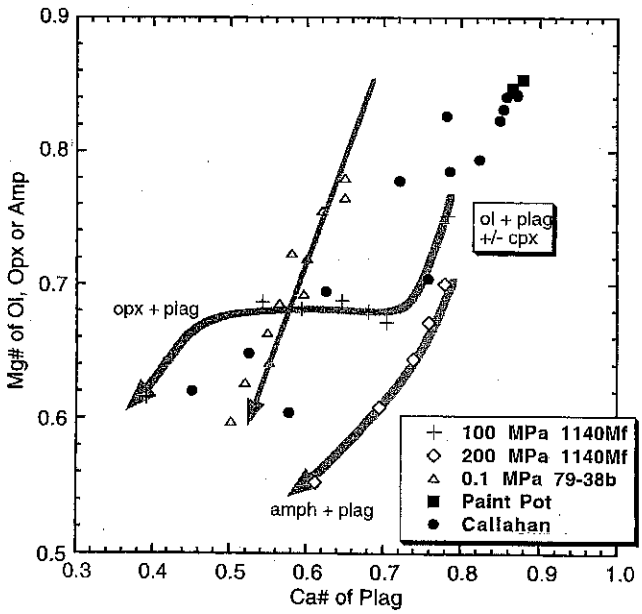

Fig. 4 Olivine–plagioclase and orthopyroxene–plagioclase co-variation in Callahan and Paint Pot Crater lavas and mineral compositional variations produced in melting experiments of Grove et al. (1997). Chemical analyses are found in Table 2

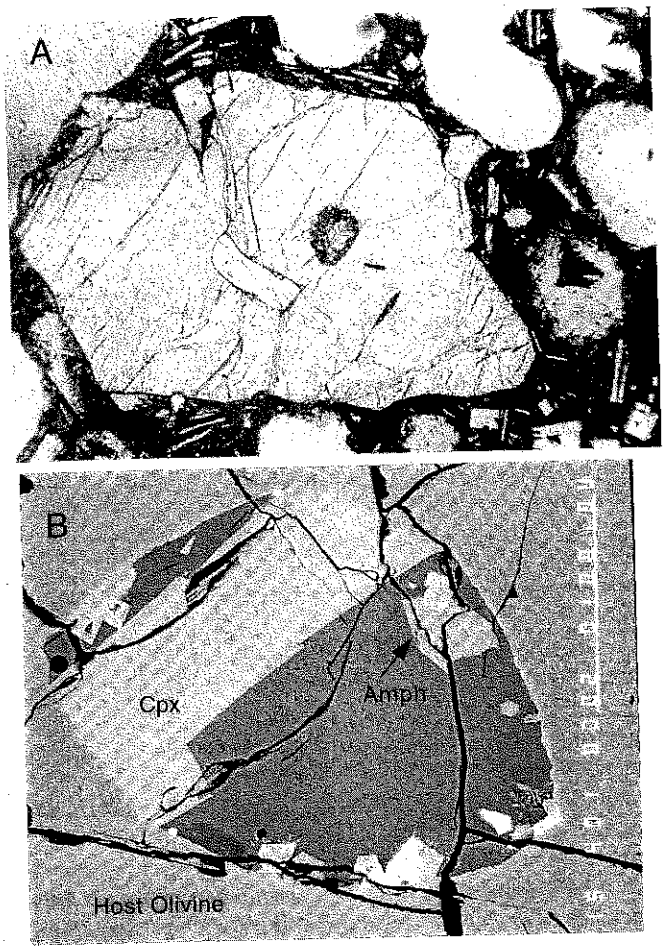

Fig. 5. A Photomicrograph of olivine phenocryst in a Paint Pot Crater lava. The olivine contains anorthite-rich plagioclase and a partly crystallized melt inclusion. Field of view is 2 mm. **B** Backscattered electron image of melt inclusion from **A**. Large grain on the *left* is high-Ca clinopyroxene. Amphibole is the *dark mineral* towards the central upper part of the inclusion. Unknown Ca-Al-Si minerals are the *brightest grains* on the right side of the inclusion. *Scale bar* is 10 μm

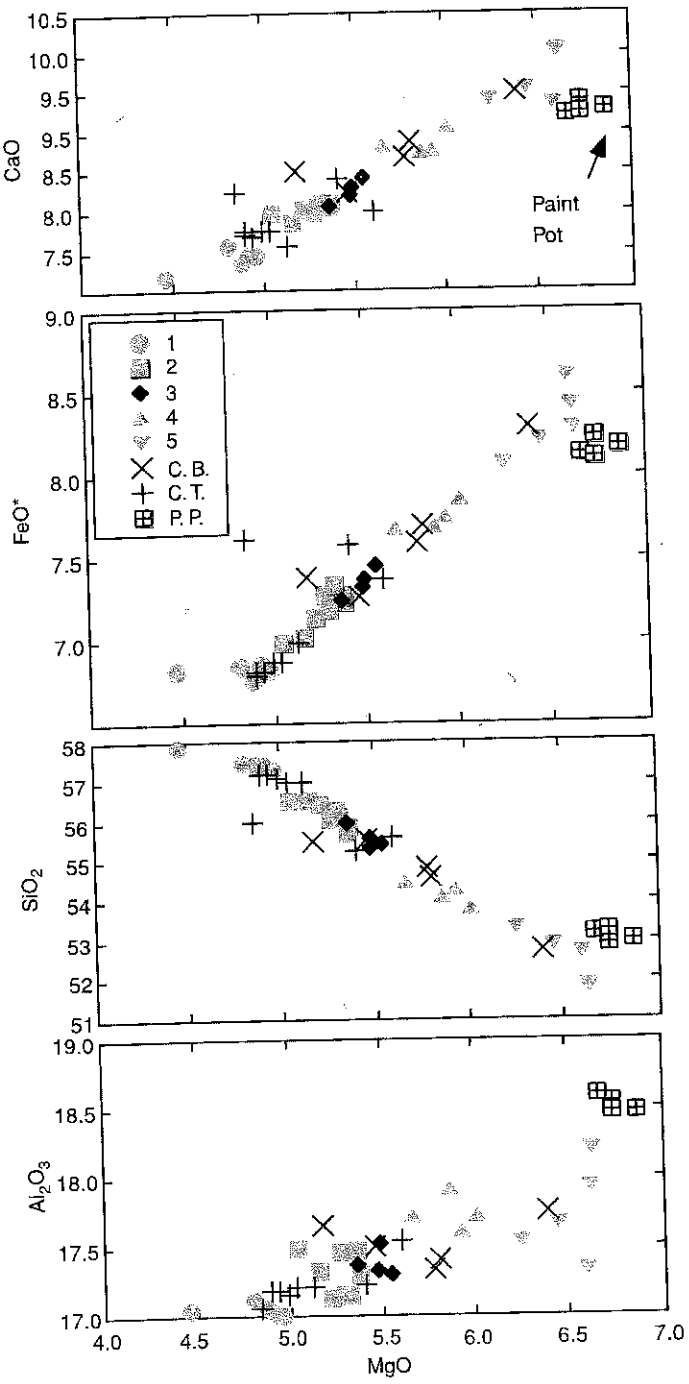

Fig. 6 Compositional variations (wt% oxides) of Callahan lava groups and tephra and the Paint Pot Crater flow lavas. Complete data set is available as electronic supplementary material at http://springer.link.de. *Symbols* for groups: 1 *grey circles*, 2 *grey squares*, 3 *black diamonds*, 4 *grey triangles*, 5 *grey triangles* with apex downwards, tephra *crosses*, Cinder Butte tephra *x*, Paint Pot Crater *square* and *cross*

olivine + plagioclase or orthopyroxene + plagioclase are compared with those from experiments in Fig. 4. For the experiments, the plotted points represent co-crystallizing phases. The mineral pairs in the lavas are analyses of crystal cores in glomerocrystic aggregates that nucleated and grew at the same time. Both Callahan and Paint Pot Crater lavas contain high An plagioclase that co-exists with the most Mg-rich olivines. Assuming that a Callahan group 5 lava represents a liquid composition, the liquidus olivine would be $Fo_{82.6}$ (using the experimentally determined $K_D^{Fe-Mg} = 0.3$ from Grove et al. 1997), and $Fo_{84.2}$ is the composition in the olivine + plagioclase glomerocrysts. For the Paint Pot Crater lavas, the calculated liquidus olivine is $Fo_{84.7}$ and the olivine co-existing with plagioclase is $Fo_{85.5}$. These olivines are good candidates for near-liquidus minerals as are the plagioclases with which they are intergrown. Since the olivine and plagioclase are intergrown, they are interpreted to have crystallized simultaneously as liquidus phases. Following similar assumptions, the Ca/Na of the most primitive Callahan and Paint Pot Crater lavas may be combined with the An content of the plagioclases in the glomerocrysts in these lavas to cal-

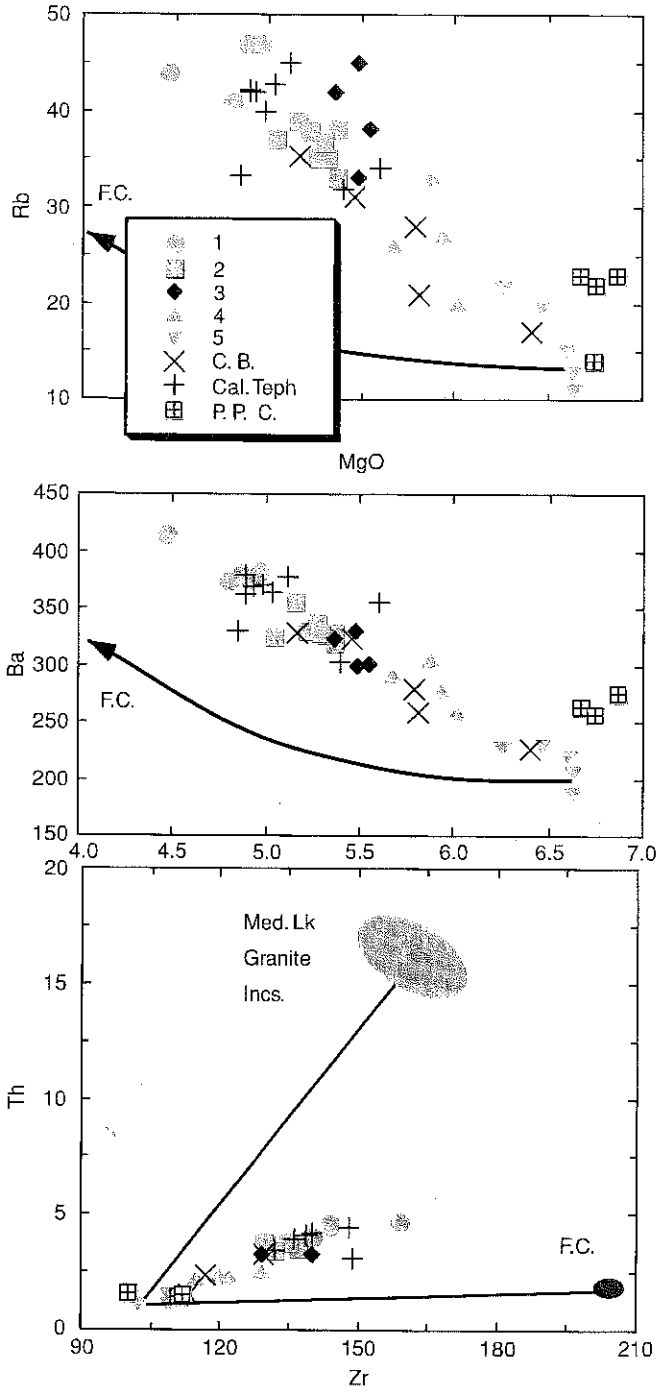

Fig. 7 Variations in trace element abundances in Callahan lava groups and tephra and in the Paint Pot Crater flow lavas. Complete data set is available as electronic supplementary material at http: // springer.link.dc. *Symbols* are the same as in Fig. 6. *Arrows* on the Rb-MgO and Ba-MgO plots indicate trends followed by fractional crystallization under hydrous conditions of 100 MPa for a group 5 parent (Table 3). *Larger ellipse* on Zr-Th plot outlines the field of Th-Zr abundances in Medicine Lake granitic inclusions (Grove et al. 1988, 1997). *Smaller darker ellipse* is the expected abundance of Th and Zr for a fractionated liquid produced under hydrous conditions from a group 5 parent (Table 3)

culate values for the $K_D^{Ca\text{-}Na}$. The range of plagioclases in the Callahan group 5 lavas co-existing with olivine is An_{85-87} and that for the Paint Pot Crater flow plagioclase is An_{87-88}. These ranges lead to calculated $K_D^{Ca\text{-}Na}$ values for the Callahan group 5 lavas of 4.0 to 4.1 and for the Paint Pot Crater lavas of 4.2 to 4.5. The value of $K_D^{Ca\text{-}Na}$ varies in response to magmatic H_2O content (Sisson and Grove 1993a). Under anhydrous conditions the value of $K_D^{Ca\text{-}Na}$ is ~1.5. At 100 MPa the value is ~3.6 (~3 wt% dissolved H_2O) and at 200 MPa, $K_D^{Ca\text{-}Na}$ is >4.0 (~6 wt% dissolved H_2O). Thus, the high values $K_D^{Ca\text{-}Na}$ estimated for the Callahan and Paint Pot Crater lavas are consistent with upper crustal crystallization under hydrous conditions for the Callahan and Paint Pot Crater lavas and appear to require pre-eruptive dissolved magmatic H_2O contents in the range of 3 to 6 wt% H_2O.

Melt inclusions in Paint Pot Crater lavas

The presence of hydrous, amphibole-bearing melt inclusions in the Mg-rich olivine of the Paint Pot Crater lavas also points to hydrous pre-eruptive crystallization conditions. The amphibole preserved in the Paint Pot Crater lavas is pargasitic and similar to that produced in the 200 MPa hydrous crystallization experiments on an andesitic inclusion from Glass Mountain (1140Mf, Grove et al. 1997). This occurrence of an olivine-hosted Paint Pot Crater lava melt inclusion is similar to one described in an older Medicine Lake lava by Mertzman (1978). Dissolved H_2O and pressure will interact to stabilize amphibole (Rutherford and Devine 1988). In the case of these olivine-hosted Paint Pot Crater lava melt inclusions, the amphibole is present in a glass that contains ~3 wt% H_2O (Table 2), which indicates a minimum pressure (H_2O saturation) of 100 MPa or depth of crystallization of ≥3 km. When compared with the H_2O estimate obtained from plagioclase, the melt inclusions indicate a slightly lower value. The lower H_2O estimate may result from differences between the conditions of melt inclusion entrapment and plagioclase crystallization. The lower H_2O content in the melt inclusion could imply trapping at lower pressures (shallower depths) during ascent of the magma prior to eruption.

Estimated fluid compositions of Callahan basaltic lavas

The hydrous lavas have distinctive trace element abundance variations that resemble those observed in other hydrous subduction zone lavas. Figure 9 shows a MORB-normalized element abundance diagram with the most primitive anhydrous Giant Crater lava (82–72f, data from Bacon et al. 1997) and the most primitive Callahan group 5 lava (1513M). The Callahan group 5 lava shows a strong enrichment in LILE abundances

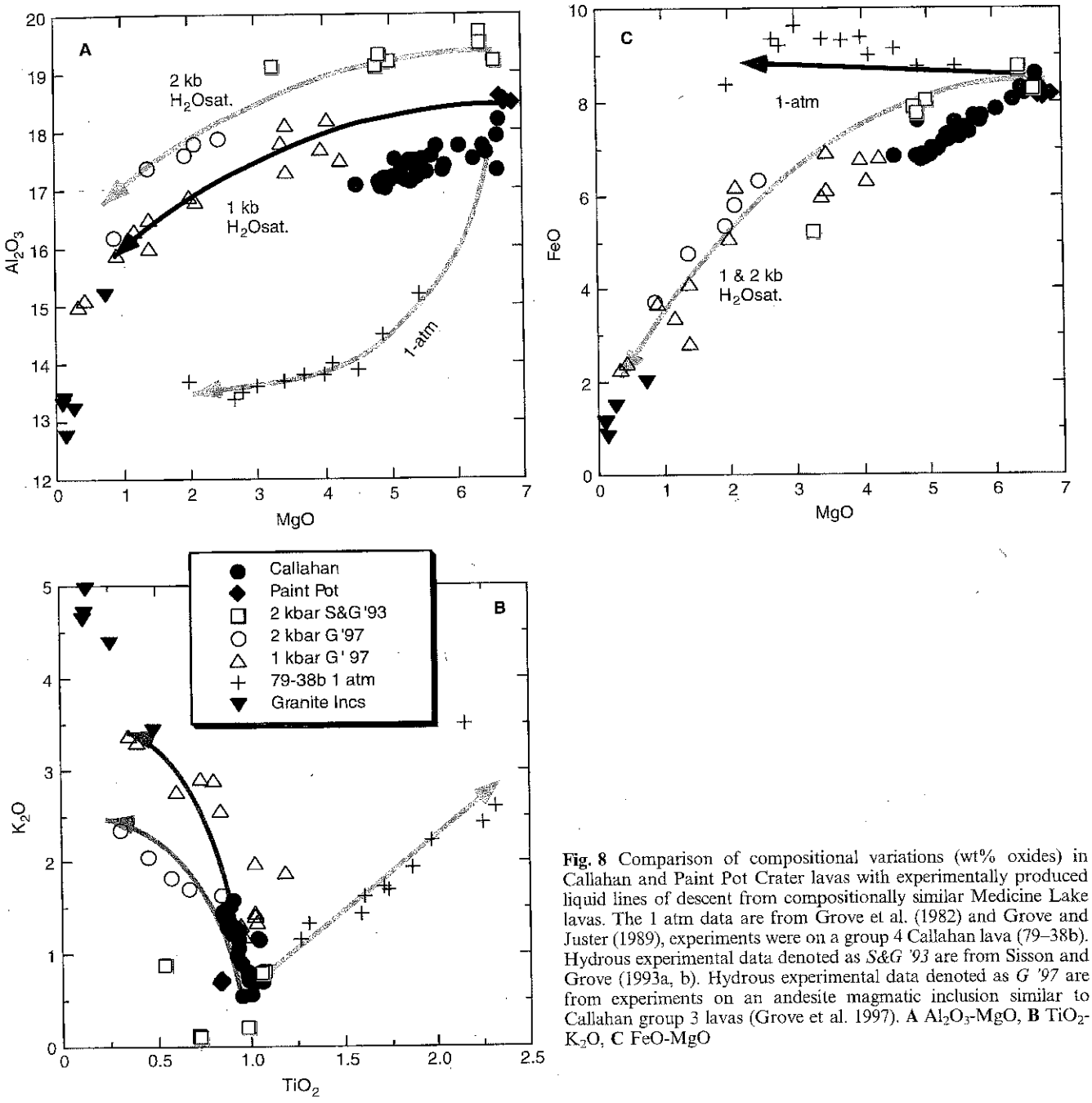

Fig. 8 Comparison of compositional variations (wt% oxides) in Callahan and Paint Pot Crater lavas with experimentally produced liquid lines of descent from compositionally similar Medicine Lake lavas. The 1 atm data are from Grove et al. (1982) and Grove and Juster (1989), experiments were on a group 4 Callahan lava (79–38b). Hydrous experimental data denoted as *S&G '93* are from Sisson and Grove (1993a, b). Hydrous experimental data denoted as *G '97* are from experiments on an andesite magmatic inclusion similar to Callahan group 3 lavas (Grove et al. 1997). **A** Al_2O_3-MgO, **B** TiO_2-K_2O, **C** FeO-MgO

(Rb, Sr, K, Ba, U and Th) relative to high field strength elements (Nb and Zr). Light rare earth elements are also enriched relative to the heavy rare earth elements. In contrast, the primitive anhydrous high alumina basalt (HAOT) has a relatively flat, MORB-like abundance pattern with the exception of a slight enrichment in LILE elements.

The contribution of a subduction-related fluid to the observed element abundances in 1513M is also shown in Fig. 9. The fluid abundance pattern was estimated by first calculating the contribution to the element abundance in 1513M by fractional melting of a depleted mantle source. For this exercise, the Hart and Zindler (1986) primitive mantle was depleted by extraction of a 1% melt. Then, the starting composition of this depleted mantle was subjected to a further episode of 15 wt% fractional melting in the garnet stability field with the melt extracted in 1% increments. The trace element composition of the aggregated fractional melt was assumed to be the contribution of the silicate mantle source region to the element abundances in 1513M. Then, the inferred pre-eruptive H_2O abundance (4 wt% H_2O) and the observed element abundance in 1513M were used to create a mass balance for the

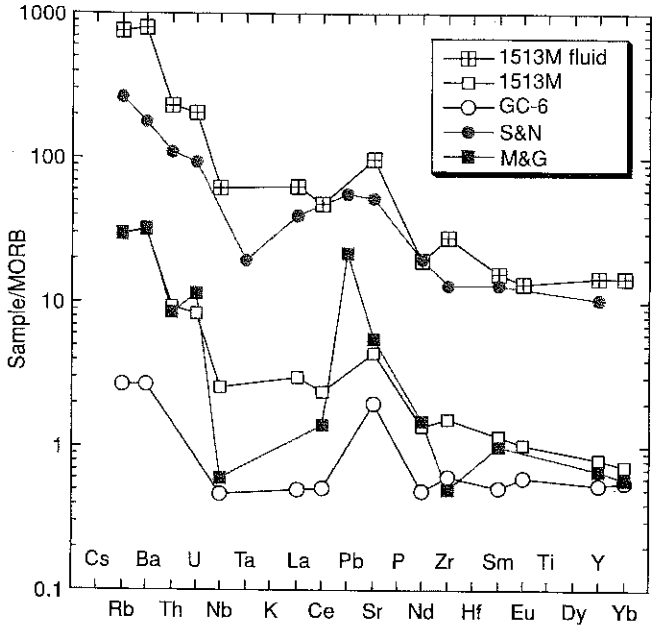

Fig. 9 Element abundance diagrams for primitive group 5, Callahan (1513M) and group 6, Giant Crater (82–72f) lavas (HAOT), and for estimates of compositions of slab-derived fluids from Stolper and Newman (1994), McCulloch and Gamble (1991) and this study (Cal Fluid, Table 3). Elements are normalized to average MORB of Sun and McDonough (1989)

element abundance in the fluid. This was accomplished using the element abundances from the silicate mantle melting model and assuming that the remaining element abundance was contributed by the subduction-related fluid. For comparison, the fluid compositions estimated for subduction-related basalts by Stolper and Newman (1994) and for island-arc basalts by McCulloch and Gamble (1991) are also shown. Note the similarity of the fluids for the Medicine Lake environment to those proposed by Stolper and Newman (1994).

Conditions of fractional crystallization and crustal assimilation

The evidence described above points to fractional crystallization under hydrous conditions as one of the processes that caused the compositional variation observed in the Callahan and Paint Pot Crater lavas. In addition, shallow level assimilation of melted silicic country rock is required to explain the elevated incompatible element abundance variations of the Callahan andesites (Fig. 7). The element abundance variations expected from fractional crystallization under hydrous conditions are shown in Fig. 7 for Rb, Ba, Th and Zr for the Callahan lavas (see Table 3 for fractional crystallization model). The lavas contain higher abundances of Rb, Ba and Th than expected for fractional crystallization and lower abundances of Zr. Grove et al. (1988, 1997) and Baker et al. (1991) discuss the role of crustal contamination in mafic Medicine Lake lavas and propose that granite underlying the volcano is the most likely assimilant. An examination of the geochemical and petrological evidence preserved in mafic eruptive products at MLV leads to the conclusion that a process involving FARM (Baker et al. 1991) operated to generate basaltic andesite and andesite at the Holocene Burnt Lava and Giant Crater flows. Evidence preserved in the chemical composition of bulk lavas and minerals in the Callahan group 1–5 lavas is also consistent with the FARM model.

Models (Table 3) were devised to test the FARM process for creating the range of magmas of the Callahan lava flow. The models use the average of the group 5 lavas as an estimate of the most mafic magmatic input, an estimated differentiate, and an assimilant represented by the granitic crustal inclusions that have been found at MLV. The differentiate is not directly represented as a sampled magma composition, but is evidenced by the presence of Fe-rich orthopyroxene + plagioclase glomerocrysts (Fig. 4) in the group 1–4 lavas. It is also shown by the Fe-Ti enriched characteristics of samples from the base of the Callahan tephra sequence (sample 1396M, Table 1). We chose several experimentally produced liquids from the 0.1 MPa anhydrous and the 100 and 200 MPa H_2O-saturated experiments that had liquid Mg# (Mg/[Mg + Fe] molar) that would be in equilibrium with the Fe-rich orthopyroxene. The major element characteristics of the groups 1 and 3 lavas were modeled by a least-squares materials balance using the major element compositions of a group 5 parent, a variety of differentiated melts, and granitic crust. Examination of the model results shows that an experimental liquid produced by fractional crystallization at 100 MPa and H_2O-saturated (1140mf No. 23) provides the best match for the differentiated liquid mixed with melted silicic crust and primitive replenished magma to create the groups 1 and 3 Callahan lavas. Thus, the mixing trends displayed by the Callahan lavas are best explained by a process that involved a hydrous composition as the differentiated melt (Fig. 8, Table 3).

To further test the mixing models we used the major element-based estimates of mixture proportions to model the abundance of several trace and rare earth elements as well as the isotopic compositions of Sr in the groups 1 and 3 andesites of the Callahan flow. The trace element abundances for the hydrous differentiated melt composition were modeled using the procedure described in Grove et al. (1997). Model assumptions and results are summarized in Table 3. The assimilant composition was assumed to be represented within the compositional range of the average granite inclusion from Medicine Lake (Grove et al. 1988) and the most mafic input was represented by the group 5 average. The mass proportions of the end member magmas, estimated using the major element least squares model for the mixed lava compositions, were used as input and the results are presented in Table 3. The match between the estimated abundances of trace and rare earth elements and the estimated isotopic compositions is close

Table 3 FARM models for Callahan lavas and an estimate of the fluid composition in hydrous mafic MLV lavas

	SiO_2	TiO_2	Al_2O_3	FeO	MgO	CaO	Na_2O	K_2O	La	Ce	Sm	Eu	Yb	Lu	Th	Ba	Rb	Zr	Sr	87/86	ΣR^2
Averages of lava groups and results of mixing models[a]																					
Average Callahan group 3 Model = 0.76 Group 5 parent +0.14 Differentiate +0.09 Assimilant																					
Lava	55.53	0.92	17.37	7.35	5.47	8.24	3.58	1.22	11	23	3.4	1.05	2.6	0.36	3.3	313	40	134	338		
Model	55.55	0.93	17.27	7.39	5.39	8.33	3.53	1.15	10	23	3.5	0.97	2.5	0.39	2.4	289	29	130	325		0.04
									10	23	3.7	1.1	2.7	0.40		291	30	131	326		
Average Callahan group 1 Model = 0.61 Group 5 parent +0.22 Differentiate +0.16 Assimilant																					
Lava	57.49	0.87	17.05	6.82	4.80	7.39	3.73	1.53	12	26	3.5	1.04	2.6	0.38	4.5	386	45	147	323	0.70372	
Model	57.51	0.89	16.13	6.82	4.69	7.51	3.66	1.45	12	26	3.7	0.92	2.6	0.40	3.3	345	39	143	305	0.70378	0.04
									12	26	4	1.15	2.9	0.42		348	40	145	307		
End members used in mixing model																					
Assimilant composition																					
Average granitic inclusion, AGI (Grove et al. 1988, Tables 8, 9, 10)																					
	73.88	0.26	14.25	1.65	0.45	1.48	3.87	4.07	23	46	4.2	0.39	2.4	0.35	13	815	144	189	157	0.70460	
708M Granitic inclusion in Paint Pot Crater (Grove et al. 1988)																					
	73.7	0.17	14.0	1.76	0.38	1.39	3.92	4.05	25	44	3.3	0.63	1.0	0.16	11	1105	163	150	170		
Liquid produced by hydrous fractional crystallization – calculated trace element abundance																					
1140Mf No. 33[b]																					
	59.9	1.11	17.1	6.55	2.78	6.08	4.46	1.68	15	35	6.3	0.98	4.7	0.61	2.4	394	32	213	292		
									14	34	4.6	2.0	3.2	0.54		383	29	207	284		
Fractionation model[c], D is used to estimate trace element abundance listed above																					
=0.14 ol+0.27 cpx + 0.58 pl									0.11	0.05	0.04	0.06	0.03	0.27	0.01	0.12	0.02	0.06	1.29		
F = 1.0 to 0.50									0.19	0.11	0.50	1.1	0.58	0.45		0.16	0.12	0.10	1.33		
Trace element composition of fluid input to Medicine Lake Volcano[d]									159	356	42	13	46	7.3	28	4997	424	2080	8730		

[a] The models assume a FARM process described by Baker et al. (1991). Parent magma is group 5 average and the differentiated magma is modeled using experimentally produced residual liquid 1140Mf No. 33 from hydrous experiments by Grove et al. (1997). This fractionated liquid is most similar to the Callahan magma that crystallized the Fe-rich orthopyroxene and Na-rich plagioclase phenocrysts in group 1. Experimentally determined mineral proportions from 100 MPa experiments are used to calculate trace element abundances of the fractionated melt using measured abundances in average Callahan group 5 (Table 1)

[b] Trace element and rare earth element abundances calculated using a fractional crystallization model described in this table in footnote c

[c] Fractionation assemblage used for the trace element modeling. Phase proportions from Grove et al. (1997). Partition coefficient sources and model assumptions: (1) tabulation of Grove and Donnelly-Nolan (1986); (2) Blundy and Wood (1991); (3) Sisson (1991); (4) Gaetani and Grove (1995); (6) Watson and Harrison (1983). The range in abundance results from the range in potential D values. Model mixes all three components. The top row of the model results shows the average group 1 or group 3 compositional data. The lower row shows the modeled FARM mixture with range of trace element abundances

[d] Estimate of the trace element composition of the fluid in hydrous mafic MLV lavas

and indicates that the mixing models provide a plausible mechanism for generating the Callahan mixed andesites. The Th-Zr co-variations (Fig. 7) illustrate the necessity of the multi-component mixing model. The liquid produced by fractional crystallization of a Callahan group 5 parent has lower Th and higher Zr than the evolved groups 1–3 andesites. Granitic crust beneath Medicine Lake has high Th and low Zr and can account for the Th-Zr systematics of the Callahan lavas, if it is used as an assimilant. It might be argued that there is another primitive parent magma that had different trace element abundances. Such a primitive parent magma may also have undergone a separate fractionation process and was then mixed with the group 5 composition. However, no magmas with these compositional characteristics have been identified at MLV.

Temporal variability in mafic Holocene magmas

The timing, conditions of magma generation, pre-eruptive conditions and nature of interactions with the shallow crust have been characterized along with the trace element and isotopic compositions of mafic and felsic magmas for many of the last 17 11,000-year eruptive events at MLV (Grove et al. 1988, 1997; Baker et al. 1990; Donnelly-Nolan et al. 1990). Four variables were selected to track the temporal variations in mafic inputs into MLV (Fig. 10): magmatic H_2O content, SiO_2 content, Sr abundance, and $^{87}Sr/^{86}Sr$ ratios. The last 11,000-year mafic magmatism at Medicine Lake is characterized by eight eruptions closely spaced in time, including a large volume eruption (~5 km^3) of high-MgO, high-alumina basalt about 10,600 ^{14}C years B.P. Low pre-eruptive H_2O, low Sr abundance, and a low $^{87}Sr/^{86}Sr$ ratio characterize this early post-glacial mafic volcanism. A 6000-year period of quiescence followed.

Volcanism recommenced with a (0.02 km^3) low-SiO_2 dacitic fissure eruption on the caldera rim about 4300 years ago. No mafic inclusions were found in this unit, but its relatively high Sr and $^{87}Sr/^{86}Sr$ suggest possible derivation from hydrous, "calc-alkaline" mafic magma. Fractionation of primitive, H_2O-poor, low-Sr basalt, similar to that which erupted at 10,600 ^{14}C years B.P. (200 ppm), cannot account for the Sr content of this aphyric dacite (340 ppm, 110M), nor could assimilation of known crustal materials. Only a single granitic inclusion among more than 30 found in Pleistocene and Holocene MLV lavas has an Sr content >300 ppm (333 ppm, 1690M). Most of the granitic inclusions contain less than 200 ppm Sr.

The next two eruptions were both H_2O-poor: the 0.001 km^3 basalt of Black Crater and Ross Chimneys (bcrc) on the north flank of the volcano and the larger (0.5 km^3) Burnt Lava andesite on the south flank. Both erupted about 3000 years ago. The basalt of Black Crater was analyzed directly for its pre-eruptive H_2O content by Sisson and Layne (1993), yielding a value of 0.1–0.3 wt%. The Burnt Lava flow contains fine grained

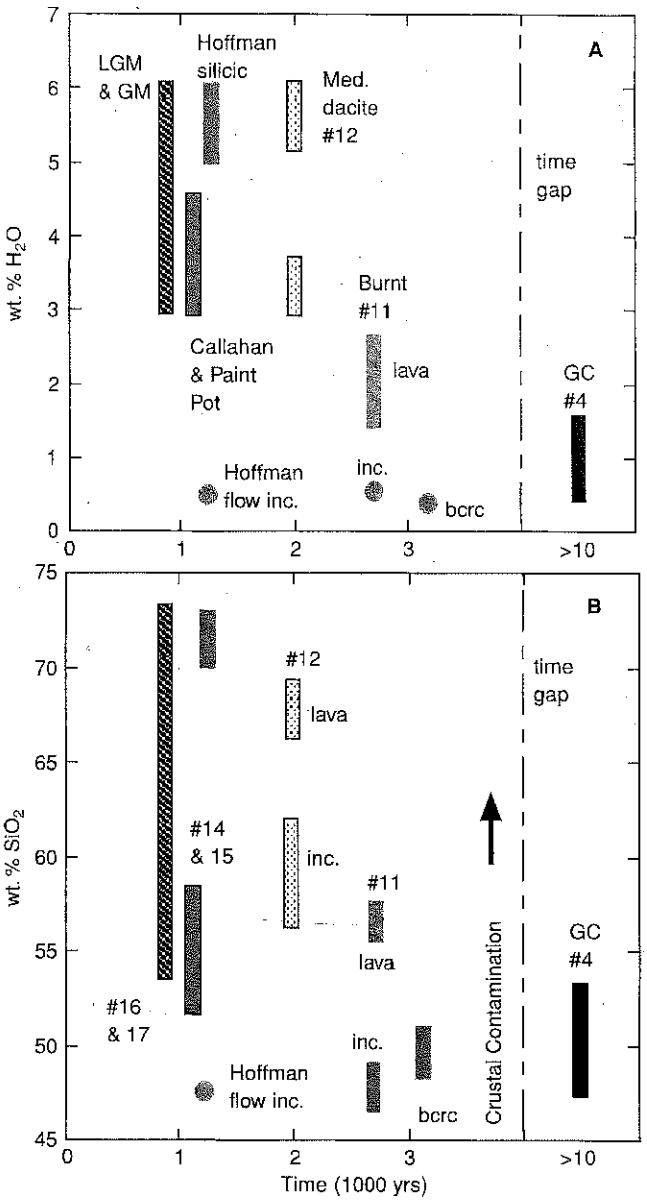

Fig. 10A–E Temporal variability in selected compositional variables for Medicine Lake lavas erupted in the last 11,000 years. *Numbering scheme* is from Fig. 2. Hoffman flow mafic inclusion is found in a rhyodacite host that is not shown in the figure. The basalt of Black Crater and Ross Chimneys is abbreviated *bcrc*. **A** wt% H_2O–time, **B** wt% SiO_2–time, **C** Sr (ppm)–time, **D** $^{87}Sr/^{86}Sr$–time and **E** $\delta^{18}O$–time

mafic magmatic inclusions with major element compositions, textures, and Sr contents (~200 ppm) like those of primitive anhydrous basalt erupted early in post-glacial time (10,600 ^{14}C years B.P.).

Another millennium intervened before eruption of the 0.08 km^3 Medicine Lake dacite flow on the caldera floor about 2000 years ago. Fine-grained andesitic magmatic inclusions from this flow have high Sr contents, including one with the highest Sr value of any eruptive product during the late Holocene (549 ppm, 1631M), suggesting a hydrous mafic source. No $^{87}Sr/^{86}Sr$ data are available for these inclusions.

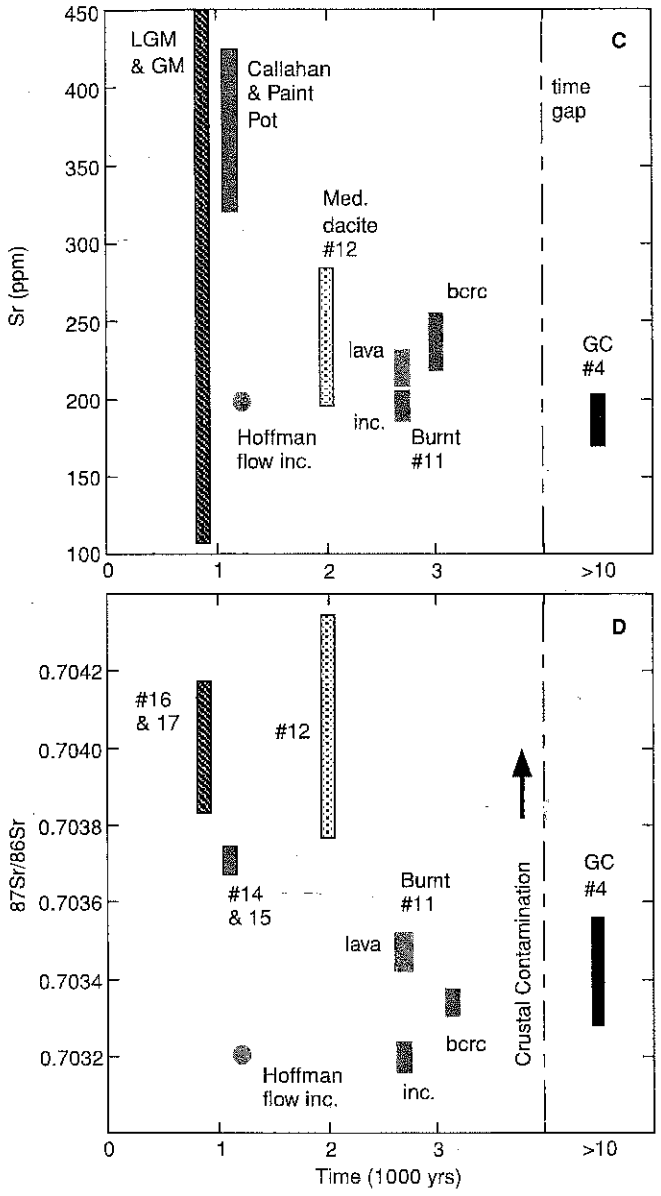

Fig. 10 (Continued)

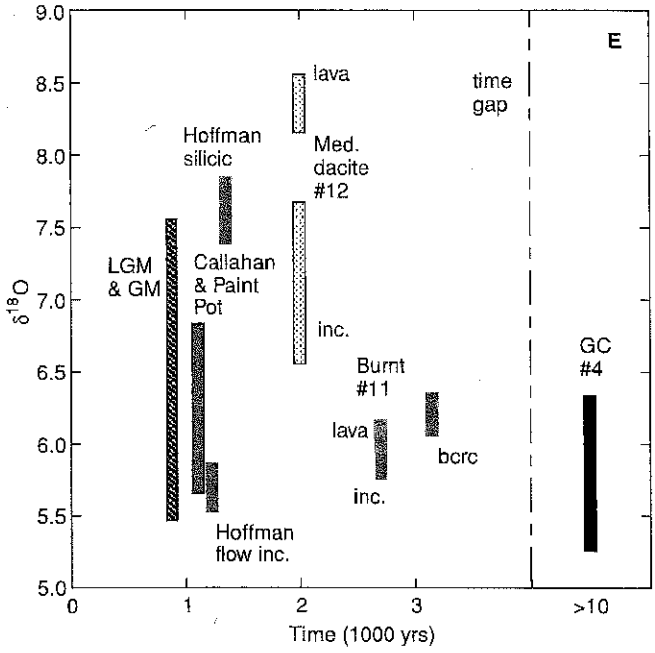

Fig. 10 (Continued)

Following another pause of about 800 years, the silicic Hoffmann flows (0.12 km^3) erupted about 1230 years ago from a fissure near the NE rim of the caldera. Fine-grained basaltic magmatic inclusions in this flow are low in Sr, similar to those in the Burnt Lava flow, indicating a probable anhydrous basaltic source for the inclusions. Thus, from about 4300 to about 1200 years before present (B.P.), mafic inputs appear to have alternated between hydrous and anhydrous.

The latest Holocene eruptive products are found to be hydrous (based on experimental, chemical and mineralogical data), with only one mafic inclusion out of dozens collected showing evidence of possible anhydrous origin. The four eruptions in latest Holocene time were the Callahan flow at about 1150 years, the Paint Pot Crater flow at 1130 years, the rhyolite of Little Glass Mountain at about 1050 years, and the rhyolite of Glass Mountain as recently as 850 years ago. Both silicic flows contain abundant fine-grained mafic magmatic inclusions that are dominantly basaltic andesite (Grove and Donnelly-Nolan 1986; Grove et al. 1997). The Sr contents of the mafic inclusions of these four eruptions range from slightly less than 300 to nearly 500 ppm, significantly higher than the 200–250 ppm Sr contents of mafic inputs thought to be H_2O-poor. The one exception is 1543M, a fine-grained andesitic rind surrounding a granitic inclusion found in the rhyolite of Glass Mountain. It contains only 218 ppm Sr. The other 40 fine-grained basaltic andesite and andesite inclusions from Glass Mountain contain 390–483 ppm Sr. Experimental evidence from a subset of these mafic inclusions (Grove et al. 1997), many of which contain amphibole, indicates dissolved water contents up to 6 wt%.

The total volume (0.5 km^3) of hydrous mafic magma erupted at MLV in late Holocene time (< 4400 years B.P.) is the same as that of H_2O-poor magma. The volume of silicic lava erupted during this same time period is about 1.5 km^3. Several lines of petrological and geochemical evidence (Grove et al. 1997; Donnelly-Nolan 1998) indicate that the rhyolites contain a large proportion of melted silicic crust (up to 50 wt% in the examples of the rhyolite of Glass Mountain and Little Glass Mountain, perhaps significantly more in the case of the Hoffmann flows and Medicine Lake dacite). The $^{87}Sr/^{86}Sr$ ratios of these silicic lavas are elevated through the incorporation of crustal material (Fig. 10). The style of interaction between the high-H_2O basalts, basaltic andesites, andesites, and shallow crust is preserved in the rhyolite and dacite flows at the Glass Mountain and Little Glass Mountain (Grove and Donnelly-Nolan

1986; Grove et al. 1997). The inclusion suite found in these flows records fractionation of hydrous primitive magmas at shallow depths (3 to 6 km) to produce rhyodacite magma. Replenishment of the magma system by hydrous mafic magma was followed by mixing in variable proportions of the replenished magma with the evolved rhyodacite magma and melted granite crust to form the dacites and rhyolites of the Glass Mountain and Little Glass Mountain.

Both the Giant Crater and the Burnt Lava systems are characterized by fractionation of H_2O-poor basalt at shallow levels to produce a high-Fe, high-Ti basaltic magma that supplied heat to melt granitic crust. Replenishment of the magmatic system by primitive high-alumina basalt mixed with the evolved Fe- and Ti-rich magma with melted granite to form the andesite of the Burnt Lava flow as well as the initial basaltic andesite of the Giant Crater lava field. The $^{87}Sr/^{86}Sr$ ratio of the andesite is elevated slightly relative to the high-alumina basalts by the incorporation of a granitic assimilant (Fig. 10).

Oxygen isotope variations

Donnelly-Nolan (1998) has shown that late Holocene lavas and inclusions are significantly higher in $\delta^{18}O$ than previously erupted lavas (Fig. 10). An increase in $\delta^{18}O$ with SiO_2 content and, for mafic lavas, with Sr content is also observed. The correlation of oxygen isotope values with chemical and isotopic indicators of hydrous mafic magmatism suggests a possible causal relationship. Donnelly-Nolan (1998) assumed that $\delta^{18}O$ values increased with increasing assimilation of granitic crustal material and concluded that a sudden shift in assimilant had occurred in late Holocene time at MLV. Another possibility is that hydrous, mafic arc magmas were derived from a mantle source with inherently higher $\delta^{18}O$ values or by a process that led to elevated $\delta^{18}O$ content. Other evidence suggests that calc-alkaline arc basalts can have elevated $\delta^{18}O$ contents despite their primitive geochemical signature (e.g. Bacon et al. 1997; Eiler et al. 1997).

In late Pleistocene time a large volume (~5 km^3), high Sr, high $\delta^{18}O$ basaltic eruption (basalt of Yellowjacket Butte, Sr 355–412 ppm, $^{87}Sr/^{86}Sr = 0.70348$, Mg# 51.7–65.3, MgO 5.79–8.23%, SiO_2 49.6–51.8%, $\delta^{18}O = +6.9$) took place on the southern flank of the volcano. This is one of the few documented exceptions to the otherwise low $\delta^{18}O$ Pleistocene lavas at MLV, but a comprehensive survey of older mafic lavas has not been attempted. The late Pleistocene Lake Basalt (3 km^3) is a high Sr, high-Al basalt that contained 4–6 wt% magmatic H_2O (Wagner et al. 1995). The basalt of Yellowjacket Butte and Lake Basalt examples and earlier high-Sr mafic lavas provide evidence that previous episodes of hydrous mafic magmatism may have occurred at MLV, but the timing, duration, and areal extent of such episodes are mostly unknown.

Temporal relationship between Holocene silicic volcanism and hydrous and anhydrous mafic inputs

Despite a large input of mafic magma (~5 km^3) about 10,600 years ago and evidence for significant crustal contamination of these primitive dry basaltic melts, no silicic lava erupted for over 6000 years. In contrast, volcanism at MLV over the last 2000 years has been dominated by high Sr, high $^{87}Sr/^{86}Sr$, and high $\delta^{18}O$ mafic and silicic lavas. Three quarters of the erupted volume in the last 2000 years has been silicic lava. Thus, there is a temporal and spatial link between the late Holocene episode of hydrous mafic magmatic input and the production of silicic melt. During both time intervals (6000 and 2000 years) mafic magmas caused significant crustal melting. In the case of the early H_2O-poor magmatic activity, the crust-magma interaction formed contaminated Fe-rich andesites with low-H_2O contents (Fig. 9a). This hybrid magma was generated because the fractionated liquids that were produced from the primitive HAOT were Fe-enriched, low-SiO_2 tholeiites (Baker et al. 1991). Mixing of melted crust, these iron-rich derivatives, and HAOT produced hybrid melts of andesitic composition (e.g. Burnt Lava flow). In the late Holocene period, hydrous mafic magma also melted shallow granitic crust, and underwent fractional crystallization. However, the liquids produced by fractional crystallization under hydrous conditions were high-SiO_2 rhyodacites (71 wt% SiO_2, Grove et al. 1997). When these silica-rich, iron-poor derivative liquids mixed with melted crust and small amounts of hydrous mafic magma, rhyolitic magmas were formed.

Relationship between elevated magmatic H_2O and arc-like geochemical signatures

The high pre-eruptive H_2O contents, isotopic and trace element characteristics of the late Holocene mafic lavas at Medicine Lake resemble lavas from nearby arc volcanic centers such as Mt. Shasta, the Lassen volcanic center, and Crater Lake (Baker et al. 1994; Bacon et al. 1997). These trace element characteristics are similar to those of other subduction-related settings, and are most likely associated with the hydrous component that was inherited from the subducted slab and mantle. Hydrous magmas at Mt. Shasta have $^{87}Sr/^{86}Sr$ and trace element characteristics that are similar to the late Holocene, hydrous magmas at MLV. Figure 11 compares Paint Pot Crater and Mt. Shasta basaltic andesites (75-SV-3 and 75-SH-317, Bacon et al. 1997). The Shasta and MLV lavas exhibit elevated LILE abundances (Sr = 604 and 354 ppm at Shasta and 500 and 350 ppm at MLV), and high La/Sm > 3. They also show high field strength element depletions, and lower heavy rare earth element abundances than primitive HAOT. Baker et al. (1994) present evidence for the presence of both hydrous and H_2O-poor mantle-derived magmas at Mt. Shasta. MLV shows evidence for the presence of hydrous and H_2O-

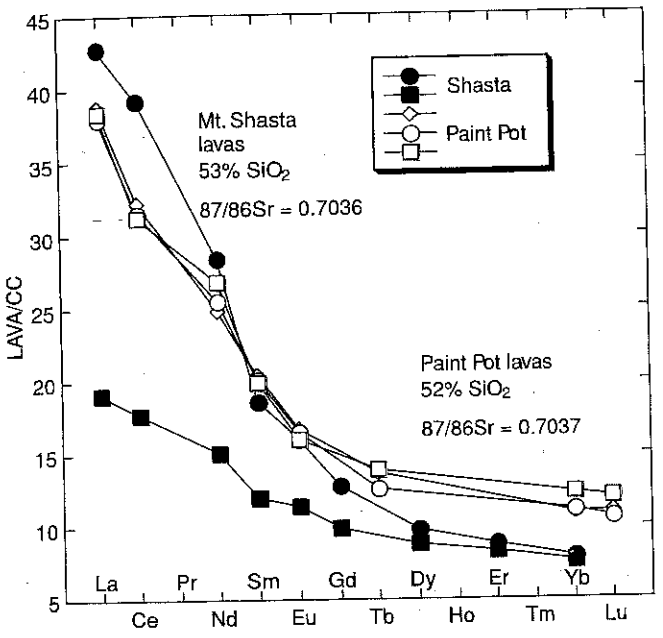

Fig. 11 Chondrite-normalized rare earth element abundances for Paint Pot Crater lavas and Mt. Shasta basaltic andesites. Data are from Bacon et al. (1997)

poor mantle-derived magmas and also provides a constraint on the time of recent transition from dominantly H_2O-poor to dominantly hydrous magmatism. The transition occurred about 2000 years ago although both dry and wet magmas were present as recently as 1230 years ago. The presence of hydrous "calc-alkaline" arc-type mafic magmas at MLV provides tangible evidence that the volcano was generated by subduction-related processes and is not simply a coincidence of location of Basin and Range volcano.

Implications for the generation of granitic magmas

The record of recent volcanism at MLV provides an interesting example of the factors that may generate granitic magmas in this continental convergent margin setting. High magmatic H_2O in basalt and andesite leads to early crystallization of Mg-Fe silicates and the suppression of plagioclase as an early crystallizing phase (Grove and Kinzler 1986). In addition, the effect of H_2O in lowering the temperature of appearance of Mg-Fe silicates on the liquidus and thereby bringing the temperature of oxide appearance closer to the liquidus (Sisson and Grove 1993a) leads to SiO_2 enrichment of residual liquids and the generation of rhyodacite-derivative liquids (Grove et al. 1997). In addition to these processes, the operation of crustal assimilation, whereby the mafic magmatic inputs provide heat to melt crust, and the replenishment by fresh inputs of mafic magma, provide the driving force to mix melted crust with differentiated SiO_2-rich magma. These combinations of processes can generate granitic magma.

This scenario is only one of many that is possible for the production of granitic melts, and it illustrates the dramatic influence of H_2O on the phase equilibrium constraints that permit SiO_2 enrichment during fractional crystallization. Obviously, the early H_2O-poor magmatism leads to the production of small volumes of rhyolite directly through crustal melting, but such rhyolite is mixed with basaltic magmas before it is erupted. In Iceland, rhyolite is produced by melting of hydrothermally altered basaltic crust that has been heated by intrusions of H_2O-poor mafic magmas (Jonasson 1994; Gunnarsson et al. 1998). According to these authors, in Iceland the wall rock is hydrothermally altered basalt, and the composition of the melt produced at the solidus is granitic. Some of the eutectic melts are segregated and erupt without interacting with mafic magmas. At MLV, however, the mafic H_2O-poor magmas are in direct contact with granitic country rock. Furthermore, fractional crystallization of the low-H_2O mafic magma is characterized by an early appearance of plagioclase as a co-crystallizing phase and late appearance of oxide minerals in the crystallization sequence. Both operate to produce high Fe, low Al_2O_3, and low SiO_2 basalts. When this iron-rich liquid is mixed with the melted crust, hybrid magmas of intermediate composition are the result. In MLV, such magmatic processes did not lead to the production of rhyolite.

Thus, geologic setting and phase equilibrium controls exercised by variations in magmatic H_2O facilitate the production of SiO_2-rich magmas. The presence of H_2O in primitive basaltic inputs beneath MLV has promoted the generation of rhyolite. Therefore, MLV provides an illustration of the suggestion that H_2O is important in the generation of granites on Earth (Campbell and Taylor 1983; Whitney 1988).

Acknowledgments The authors thank C. Bacon, G. Bergantz, R. Lange and T. Sisson for careful and thoughtful reviews. This research was supported by NSF grant EAR9706214.

References

Albee AL, Ray L (1970) Correction factors for electron probe microanalysis of silicates, oxides, carbonates, phosphates and sulfates. Anal Chem 42: 1408–1414

Anderson CA (1933) Volcanic history of Glass Mountain, northern California. Am J Sci 26: 485–506

Bacon CR, Bruggman PE, Christiansen RL, Clynne MA, Donnelly-Nolan JM, Hildreth W (1997) Primitive magmas at five Cascade volcanic fields: melts from hot, heterogeneous sub-arc mantle. Can Mineral 35: 397–423

Baker MB, Grove TL, Kinzler RJ, Donnelly-Nolan JM, Wandless GA (1991) Origin of compositional zonation (high-alumina basalt to basaltic andesite) in the Giant Crater lava field, Medicine Lake volcano, northern California. J Geophys Res 96: 21819–21842

Baker MB, Grove TL, Price R (1994) Primitive basalts and andesites from the Mt. Shasta region, N. California: products of varying melt fraction and water content. Contrib Mineral Petrol 118: 111–129

Bartels KS, Kinzler RJ, Grove TL (1991) High pressure phase relations of primitive high-alumina basalts from Medicine Lake, northern California. Contrib Mineral Petrol 108: 253–270

Bence AE, Albee AL (1968) Empirical correction factors for the electron microanalysis of silicates and oxides. J Geol 76: 382–403

Blundy JD, Wood BJ (1991) Crystal-chemical controls on the partitioning of Sr and Ba between plagioclase feldspar, silicate melt and hydrothermal solutions. Geochim Cosmochim Acta 55: 193–208

Campbell IH, Taylor SR (1983) No water, no granites- no oceans, no continents. Geophys Res Lett 10: 1061–1064

Condie KC, Hayslip DL (1975) Young bimodal volcanism at Medicine Lake volcanic center, northern California. Geochim Cosmochim Acta 39: 1165–1178

Donnelly-Nolan JM (1988) A magmatic model of Medicine Lake volcano, California. J Geophys Res 93: 4412–4420

Donnelly-Nolan JM (1998) Abrupt shift in $\delta^{18}O$ values at Medicine Lake volcano, CA. Bull Volcanol 59: 529–536

Donnelly-Nolan JM, Champion DE, Miller CD, Grove TL, Trimble DA (1990) Post-11,000-year volcanism at Medicine Lake volcano, Cascade Range, northern California. J Geophys Res 95: 19693–19704

Eichelberger JC (1975) Origin of andesite and dacite: evidence of mixing at Glass Mountain in California and at other circum-Pacific volcanoes. Geol Soc Am Bull 86: 1291–1381

Eiler JM, McInnes BIA, Valley JW, Graham CW, Stolper EM (1997) Slab-derived fluids in the mantle: oxygen-isotope evidence from melt inclusions. 7th Annu VM Goldschmidt Conf, LPI Contrib 921: 65–66

Gaetani GA, Grove TL (1995) Partitioning of rare-earth elements between clinopyroxene and silicate melt: crystal-chemical controls. Geochim Cosmochim Acta 59: 1951–1962

Gerlach DC, Grove TL (1982) Petrology of Medicine Lake Highland Volcanics: characterization of end members of magma mixing. Contrib Mineral Petrol 80: 147–159

Grove TL, Donnelly-Nolan JM (1986) The evolution of young silicic lavas at Medicine Lake volcano, California: implications for the origin of compositional gaps in calc-alkaline series lavas. Contrib Mineral Petrol 92: 281–302

Grove TL, Kinzler RJ (1986) Petrogenesis of andesites. Annu Rev Earth Planet Sci 14: 417–454

Grove TL, Juster TC (1989) Experimental investigations of low-Ca pyroxene stability and olivine-pyroxene-liquid equilibria at 1-atm in natural basaltic and andesitic liquids. Contrib Mineral Petrol 103: 287–305

Grove TL, Gerlach DC, Sando TW (1982) Origin of calc-alkaline series lavas at Medicine Lake volcano by fractionation, assimilation and mixing. Contrib Mineral Petrol 80: 162–180

Grove TL, Kinzler RJ, Baker MB, Donnelly-Nolan JM, Lesher CE (1988) Assimilation of granite by basaltic magma at Burnt Lava flow, Medicine Lake volcano, northern California: decoupling of heat and mass transfer. Contrib Mineral Petrol 99: 320–343

Grove TL, Donnelly-Nolan JM, Housh T (1997) Magmatic processes that generated the rhyolite of Glass Mountain, Medicine Lake volcano, N. California. Contrib Mineral Petrol 127: 205–223

Gunnarsson B, Marsh BD, Taylor HP Jr (1998) Generation of Icelandic rhyolites: silicic lavas from the Torfajokull central volcano. J Volcanol Geotherm Res 83: 1–45

Hart SR, Zindler A (1986) In Search of a bulk-earth composition. Chem Geol 57: 247–267

Jonasson K (1994) Rhyolite volcanism in the Krafla central volcano. Bull Volcanol 56: 516–528

Mertzman SA Jr (1977) Recent volcanism at Schonchin and Cinder Buttes, northern California. Contrib Mineral Petrol 61: 231–243

Mertzman SA Jr (1978) A Tschermakite-bearing high-alumina olivine tholeiite from the southern Cascades, California. Contrib Mineral Petrol 67: 261–265

Mertzman SA Jr (1979) Strontium isotope geochemistry of a low potassium tholeiite and two basalt-pyroxene andesite magma series from the Medicine Lake Highland, California. Contrib Mineral Petrol 70: 81–88

McCulloch MT, Gamble JA (1991) Geochemical and geodynamical constraints on subduction zone magmatism. Earth Planet Sci Lett 102: 358–374

Rutherford MJ, Devine JD (1988)) The May 18, 1980 eruption of Mt. St. Helens 3. Stability and chemistry of amphibole in the magma chamber. J Geophys Res 93: 11949–11959

Sisson TW (1991) Pyroxene-high silica rhyolite trace element partition coefficients measured by ion microprobe. Geochim Cosmochim Acta 55: 1575–1585

Sisson TW, Grove TL (1993a) Experimental investigations of the role of water in calc-alkaline differentiation and subduction zone magmatism. Contrib Mineral Petrol 113: 143–166

Sisson TW, Grove TL (1993b) Temperature and H_2O contents of low-MgO high-alumina basalts. Contrib Mineral Petrol 113: 167–184

Sisson TW, Layne GD (1993) H_2O in basalt and basaltic and andesite glass inclusions from four subduction-related volcanoes. Earth Planet Sci Lett 117: 619–635

Smith AL, Carmichael ISE (1968) Quaternary lavas from the southern Cascades, western USA. Contrib Mineral Petrol 19: 212–238

Stolper E, Newman S (1994) The role of water in the petrogenesis of Mariana Trough magmas. Earth Planet Sci Lett 121: 293–325

Sun SS, McDonough WD (1989) Chemical and isotopic systematics of oceanic basalts: implications for mantle compositions and processes. In: Saunders AD, Norry MJ (eds) Magmatism in the ocean basins. Geol Soc Lond Spec Pub 42: 313–345

Wagner TP, Donnelly-Nolan JM, Grove TL (1995) Evidence of hydrous differentiation and crystal accumulation in the low-MgO, high-Al_2O_3 Lake Basalt from Medicine Lake volcano, California. Contrib Mineral Petrol 121: 201–216

Watson EB, Harrison TM (1983) Zircon saturation revisited: temperature and composition effects in a variety of crustal magma types. Earth Planet Sci Lett 64: 295–304

Whitney JA (1988) The origin of granite: the role of source water in the evolution of granitic magmas. Geol Soc Am Bull 100: 1886–1897